

FE modeling of Partially Steel-Jacketed (PSJ) RC columns using CDP model

Marco F. Ferrotto¹, Liborio Cavaleri^{*1} and Fabio Di Trapani²

¹Department of Civil, Environmental, Aerospace, Materials Engineering, University of Palermo, Palermo, Italy

²Department of Structural, Geotechnical and Building Engineering, Polytechnic of Turin, Italy

(Received February 23, 2018, Revised April 26, 2018, Accepted May 23, 2018)

Abstract. This paper deepens the finite element modeling (FEM) method to reproduce the compressive behavior of partially steel-jacketed (PSJ) RC columns by means of the Concrete Damaged Plasticity (CDP) Model available in ABAQUS software. Although the efficiency of the CDP model is widely proven for reinforced concrete columns at low confining pressure, when the confinement level becomes high the standard plasticity parameters may not be suitable to obtain reliable results. This paper deals with these limitations and presents an analytically based strategy to fix the parameters of the Concrete Damaged Plasticity (CDP) model. Focusing on a realistic prediction of load-bearing capacity of PSJ RC columns subjected to monotonic compressive loads, a new strain hardening/softening function is developed for confined concrete coupled with the evaluation of the dilation angle including effects of confinement. Moreover, a simplified efficient modeling approach is proposed to take into account also the response of the steel angle in compression. The prediction accuracy from the current model is compared with that of existing experimental data obtained from a wide range of mechanical confinement ratio.

Keywords: ABAQUS; confined concrete; concrete damaged plasticity; steel jacketing

1. Introduction

Advances in seismic rehabilitation of existing structures gained in the last decade require the need of powerful computational tools able to perform reliable assessment of structural capacity of RC members before and after strengthening.

Finite Element (FE) software such as ABAQUS offers several efficient methods to capture mechanical behavior of reinforced concrete (RC) members and/or masonry structures subjected to several load conditions as for static and dynamic loads or time-dependent effects (Jin *et al.* 2007, Chen *et al.* 2012, Barasan 2015, Genikomsou and Polak 2015, Mahdikhani *et al.* 2016). Moreover, the enhancement of strength and strain properties of RC columns subjected to strengthening can be efficiently analyzed by means of accurate numerical analyses performed by this FE software.

Among the most used retrofitting techniques, strengthening of existing RC columns by means of external steel cages results an efficient and reliable method for the improvement of load-bearing and deformational capacity. This kind of strengthening technique is realized by applying at the corners of square or rectangular RC columns steel angles to which steel battens are usually welded to provide confinement of the concrete. The improvement of a member due to confinement is generally coupled with the axial load contribution of the vertical steel angles that, based on the presence or not of mechanical connection with the slabs, it can be provided directly or indirectly by friction (Campione

et al. 2017).

Several analytical studies were developed to predict the compressive behavior of a strengthened column according to experimental results (Montuori and Piluso 2009, Badalamenti *et al.* 2010, Tarabia *et al.* 2014, Campione *et al.* 2016). However, the complex nature of the confinement action for partially steel-jacketed (PSJ) RC columns requires the need of accurate prediction of the capacity not always achievable from analytical or plane-section numerical models. The non-uniform strain distribution along the height of the columns during compression loads causes a progressive yielding of the horizontal steel plates so that the confinement mechanism strongly depends on the expansion of the concrete at each section of the column.

Although many researchers have published studies regarding the experimental behavior and FE modeling of FRP-confined concrete columns, skeletal structures or shear walls (Yu *et al.* 2010, Hany *et al.* 2016, Behfarnia and Shirmeshan 2017, Chen *et al.* 2015, 2017, Ferrotto *et al.* 2017, Chi *et al.* 2017) and concrete-filled steel stub columns (Han *et al.* 2007, Tao *et al.* 2013, Gupta *et al.* 2015, Hoang and Fehling 2017), there is a lack in the studies for PSJ RC columns. Further, the use of CDP model to reproduce the compressive response of confined concrete of such columns is worthy of many more considerations.

The common point of view of the various authors that investigated on this issue is that the default parameters usually adopted for concrete subjected to low confining pressure such as for internal steel reinforcement lead to a non-realistic prediction of the compressive capacity for concrete subjected to high confining pressure as it happens when the existing columns are strengthened with the techniques above described. On this regard, this paper is aimed to fill this lack and provide a reliable prediction tool

*Corresponding author, Professor
E-mail: liborio.cavaleri@unipa.it

for the definition of the plasticity parameters of concrete under multi-axial stresses.

2. Finite element modeling

The finite element software ABAQUS CAE version 6.13 was used to build a FE model of reinforced concrete columns, with square or rectangular cross-sections, externally confined with steel angles and plates.

The column and the steel cage were modeled with C3D8-R elements (8-node linear brick, reduced integration, hourglass control), while the internal steel reinforcement was modeled with T3D2 elements (2-node linear 3-D truss). Mesh convergence studies were carried out to observe the influence of the aspect ratio of the C3D8-R elements on the global response and to determine optimal FE mesh that provides relatively accurate solution with low computational efforts. Elements with aspect ratio not higher than 1.5 resulted optimal for the numerical simulations.

2.1 Boundary conditions and interaction

To simulate the boundary conditions, two rigid bodies at the top and the bottom of the specimen with the translational degrees of freedom restrained for the ends except for the vertical displacement (direction of loading) were defined.

The internal steel reinforcement was considered as “embedded element” in the concrete column which acts as a “host element” whose response is used to constrain the translational degrees of freedom of the embedded nodes. This strategy reasonably assumes that no sliding between internal steel and concrete occurs under compression.

“Tie-constrain” interactions were used to define the contact properties between the steel battens and the steel angles to simulate the welding of the steel so that there was no relative motion between them. The same interactions were defined also between the concrete column and the steel angles.

The latter assumption allows to define a perfect contact between steel angles and concrete (avoiding potential convergence problems due to other types of contact modeling) provided that an adequate material constitutive law is defined for the steel angles as it is explained in the next section.

2.2 Material modelling of steel

During compression tests, RC Steel Jacketed columns are usually loaded in two different ways, that are applying the load both to the steel angles and the concrete (angles fully-loaded) or to the concrete column only (angles indirectly-loaded). Of course, the global response will be affected by the load conditions.

Several researches in the last years demonstrated that in the case of angles fully-loaded the compressive response of the steel can be affected by buckling. This effect can be restrained depending on the spacing of the horizontal steel battens.

In the proposed FE model, buckling effects for the steel

angles are indirectly considered assigning constitutive stress-strain law to the steel according to a well assessed analytical model provided by Badalamenti *et al.* (2010). The model considers the critical compressive stress of the angles depending on the ultimate bending moment of the angle subjected to axial force, axial bending and lateral loads q , the latter assumed equivalent to the lateral confinement pressure f_{le} provided by the horizontal steel battens. The critical stress is evaluated as

$$\sigma_c = \frac{1}{s_b \cdot l_t \cdot t} \cdot \frac{1}{\sqrt{2\varepsilon_s - \varepsilon_s^2}} \cdot \left\{ 2 \left[\frac{l_t^2 \cdot t \cdot f_{yb}}{4} - \frac{(N_u^*)^2}{16f_{yb} \cdot t} \right] - \sqrt{2} f_{le} \cdot l_t \frac{s_b^2}{4} \right\} \quad (1)$$

$$N_u^* = \varepsilon_s \cdot 2 \cdot l_t \cdot t \cdot E_s \leq 2 \cdot l_t \cdot t \cdot f_{yb} \quad (2)$$

with s_b being the spacing of the horizontal steel battens, l_t the transversal width of the angles, t the thickness of the angles, ε_s the axial strain of the angle.

The axial stress-strain law for the angles including buckling effects is

$$\sigma_s = \begin{cases} \min(E_s \varepsilon_s; \sigma_c) & \varepsilon_s \leq \varepsilon_{yb} \\ \min(f_{yb}; \sigma_c) & \varepsilon_s > \varepsilon_{yb} \end{cases} \quad (3)$$

For more details, refer to the original paper provided by the authors.

Conversely, if the angles are not in contact with the end rigid plates (simulating the slabs) of the load-testing machine (angles indirectly-loaded) friction occurs between the steel and the concrete column. In this paper, the effect of sliding between angles and concrete is indirectly considered assuming a reduced limit stress of the steel angles since tie-constraints are used between angles and concrete.

In this case, Campione *et al.* (2017) suggested to evaluate an equivalent axial compressive stress to be assigned to the angles if they are included in a plane-fiber section model considering the tangential stresses along the contact surfaces as a function of the cohesion c_0 , of the friction μ between steel and concrete and of the lateral confinement pressure f_{le} provided by the steel battens. The limit normal stress for the cross sections of the angles is

$$f_y^* = \frac{2 \cdot l_t \cdot l_0}{t(2 \cdot l_t - t)} (c_0 + \mu \cdot f_{le}) \quad (4)$$

where l_t is the transversal width of the angles, l_0 is the length of the angles in contact with the column and t is the thickness of the angles. Moreover, the authors suggested to express the axial compressive stress-strain for the angles including friction effects as

$$\sigma_s = \min \left\{ \frac{f_y^*}{\varepsilon_{c0}} \varepsilon_s; f_y^* \right\} \quad (5)$$

In Eq. (5), ε_{c0} is the strain at peak strength of concrete in the unconfined state. This empirical value was adopted by the authors based on the observation of the experimental tests, resulting suitable in the reproduction of the experimental results without the need to model the interface

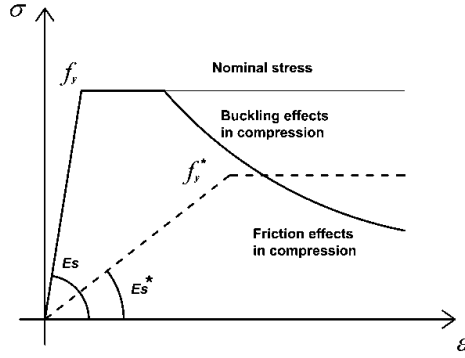


Fig. 1 Axial stress-strain response of steel angles in compression

behavior between steel angles and concrete according to the plane-fiber section modeling approach. Moreover, the value of the friction μ , not directly used but considered for the definition of the stress-strain law of the steel angles to be used in the FE model, was 0.4 coupled with a value of the cohesion c_0 of 0.1 MPa (if mortar is used between steel angles and concrete, otherwise $c_0=0$) according to the suggestions of Campione *et al.* (2017).

In Fig 1 the compressive stress-strain response of the steel angles is shown for the two load conditions (angles directly and indirectly loaded).

2.3 Material modeling of concrete

There are different models allowing to define the non-linear mechanical behavior of concrete with the ABAQUS software. Drucker-Prager (D-P) type plasticity model and Concrete Damaged Plasticity Model (CDP) are the most reliable models among all the available options of the software. According to the *plasticity theory* the nonlinear behavior of the concrete is identified by three key components: the *yield criterion*, the *hardening/softening rule* and the *flow rule*. More advantages however are achievable by using CDP model thanks to the possibility to take into account the damage effects including the reduction of the elastic stiffness during the loading process for monotonic and cyclic loads. In the present work, CDP model was used to perform simulation in the case of confinement under monotonic loads only, therefore the damage variables were not defined and the concrete was modeled as plasticity only.

The elastic behavior of the concrete is managed by defining the Poisson ratio ν_c (with a representative value of 0.2 in most cases) and the modulus of elasticity E_c , assumed in this study depending on the unconfined concrete compressive strength (ACI 318) as $E_c = 4730 \sqrt{f_{c0}}$.

In the present work, the strain at unconfined concrete strength ε_{c0} was evaluated according to De Nicolò *et al.* (1994) based on a regression analysis of uniaxial compression tests resulting from 17 references, in which f_{c0} ranged from 10 MPa to 100 MPa (because of its reliability, this equation was also used by Tao *et al.* (2013))

$$\varepsilon_{c0} = 0.00076 + \sqrt{(0.626 f_{c0}) \cdot 10^{-7}} \quad (6)$$

2.3.1 Concrete damaged plasticity model

By using the plasticity model available in ABAQUS, it is possible to take into account concrete cracking in tension as well as crushing in compression. Formulations defining the behavior of concrete under multi-axial stress state include the *yield criterion*, the *flow rule* and the *hardening/softening rule* that defines the non-linear behavior of concrete.

The above formulations can be managed in ABAQUS (Abaqus Theory and User manuals, 2013) by the users defining the *plasticity parameters*. These are the dilation angle ψ that defines the plastic flow potential, the ratio between the compressive strength under biaxial loading and uni-axial compressive strength f_{b0}/f_{c0} , the flow potential eccentricity e , the viscosity parameter μ and the ratio K_c between the second stress invariant on the tensile meridian and that on the compressive meridian for the yield function.

In this work, the tension stiffening is defined according to Tao *et al.* (2013), with linear uniaxial tensile stress for the concrete up to the reaching of the tensile strength assumed of 0.1 of f_{c0} . The softening response is then defined by means of fracture energy G_f depending on the uniaxial compressive strength f_{c0} and the maximum coarse aggregate size d_0 (assumed 20 mm if no specified)

$$G_f = (0.0469d_0^2 - 0.5d_0 + 26)(0.1f_{c0})^{0.7} \quad [N/m] \quad (7)$$

The CDP model can be considered a powerful tool for the prediction of the reinforced concrete response under low confining pressures, as in the case of RC members of general structures interest. However, constant default values could not be suitable to be used in some case due to the nature of the tri-axial stress state of the concrete when the confining pressure become high as for external FRP or steel wrapped concrete columns. In the following, based on a sensitivity analysis, the influence of the plasticity parameters in the evaluation of the load-strain response of PSJ-concrete columns is analyzed.

The FE model built for the sensitive analysis consisted in a square section concrete column having base b of 200 mm and height h of 750 mm. The uniaxial concrete compressive strength f_{c0} was assumed of 30 MPa. The column was externally confined with steel angles and plates having dimension of 50/50/5 and 40/4 with yield stress of 275 MPa. The hardening/softening function was preliminary adopted by assuming the uniaxial stress-strain law for the unconfined concrete according to Popovics (1973). However, for confined specimens, a hardening/softening function different from that used for unconfined specimens should be adopted to obtain more accurate results as it will be shown later.

In Figs. 2(a)-(d) the “as built model”, the meshing and the stress and strain fields for a generic step of analysis performed for compression loads are shown respectively.

2.3.2 Influence of the plasticity parameters on the load-bearing capacity

No particular changes were observed in the evaluation of the compressive behavior by varying the default value for the flow potential eccentricity e and the viscosity μ , therefore, the default values of 0.1 and 0 were assumed

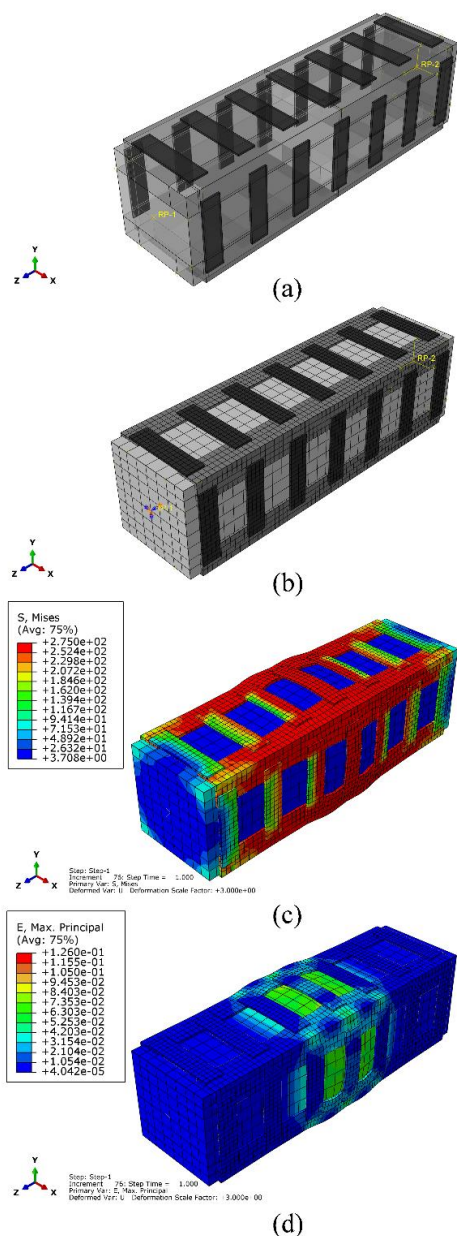


Fig. 2 “As built model” (a); Meshing (b), Stress field (c), Strain field (d)

according to other researches.

The ratio between the second stress invariant on the tensile meridian and that on the compressive meridian (K_c) is one of the parameters for determining the yield surface of concrete plasticity model. K_c can take values from 0.5 to 1 (triangular shape to circular shape of the yield surface). The default value for normal strength concrete of K_c is 0.667, but, as demonstrated by several authors, this value could be not suitable to be used for each type of concrete. Yu *et al.* (2010) assumed $K_c = 0.725$ as a recommended value for FRP-confined concrete columns subjected to monotonic compressive load if the model of Teng *et al.* (2007) is used to evaluate the strength of the confined concrete. Tao *et al.* (2013) proposed for CFST columns to evaluate K_c depending on the uniaxial concrete strength f_{c0} if the ratio f_{b0}/f_{c0} is evaluated according to Papanikolaou and Kappos

(2007) (f_{b0} is the biaxial concrete strength). This assumption was adopted also by Hany *et al.* (2016) coupled with the hypothesis of Yu *et al.* (2010) regarding the adoption of the model of Teng *et al.* (2007) for the strength of FRP-confined concrete.

In Fig. 3(a), the influence of K_c on the axial stress-strain response is shown for values of K_c of 0.55, 0.6, 0.667, 0.7, 0.8, 1 for a given value of the dilation angle ψ assumed equal to 30° , that is the default value. The compressive capacity is considerably influenced by the value of K_c , especially in the range of 0.5-0.7, confirming that K_c should be evaluated very carefully.

The dilation angle ψ is the only parameter that affects the lateral strain-axial strain curve, defining the plastic flow potential. The allowed values for ψ range from 0° to 56° . Different authors in the past assumed for normal strength concrete constant values between 20° and 30° independently from the nature and the confinement level. In this work, a sensitive analysis is performed for ψ values of 0.1° , 10° , 20° , 40° , 56° to observe the influences on the stress-strain response of the confined concrete by means of the same column previously used to investigate on the effects of K_c . The value of K_c was assumed in this phase according to previous studies as for Yu *et al.* (2010), Teng *et al.* (2013), Hany *et al.* (2016).

The results indicate that the dilation angle strongly influences the compression capacity of the confined concrete (Fig. 3(b)). For values of ψ lower than 20° the confined compressive strength resulted even lower of the input value f_{c0} . Moreover, convergences problems occurred during numerical simulations.

In detail, the first stages of the stress-strain response are not affected by the dilation angle. Beyond compressive stress values of about 0.7 of f_{c0} the differences become significant, showing that the strength increases as the dilation angle increases. This effect is physically consistent with the confinement mechanism for which with higher confinement levels, strongly interaction is developed between the concrete and the confining device, resulting in higher compressive capacity. However, by increasing the dilation angle, although the strength increase, almost identical slopes are obtained in the softening branch. This aspect is not consistent with experimental results for which, by increasing the confinement level, the slope of the softening become lesser with benefit on the ductility of the composite members.

In the present model, K_c was evaluated depending on the ratio f_{b0}/f_{c0} according to Ozbakkaloglu *et al.* (2016) on the basis of a large experimental database of specimens with f_{c0} from 10 to 100 MPa. Based on a power regression analysis, they proposed

$$\frac{f_{b0}}{f_{c0}} = 1.57 \cdot f_{c0}^{-0.09} \quad (8)$$

In doing so, K_c can be evaluated as

$$K_c = 0.71 \cdot f_{c0}^{-0.025} \quad (9)$$

2.3.3 Modification proposal

What above described highlights the need to an accurate

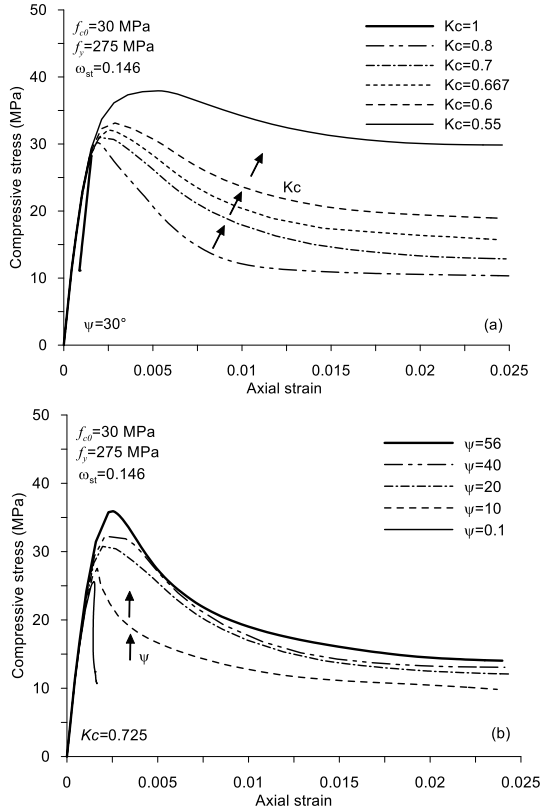


Fig. 3 Influence of K_c (a) and ψ (b) on the axial stress-strain response

definition of the plasticity parameters to be used for CDP model in ABAQUS to provide a reliable prediction tool for the capacity evaluation of PSJ-columns subjected to monotonic compressive loads.

Regarding the hardening/softening function, it should be noted that different authors provided in the last period several approaches to evaluate adequate uniaxial constitutive laws for concrete to cope the limitation on the prediction of the confined concrete after the peak stress. Among the most relevant studies, Adam *et al.* (2007), by using ANSYS software, proposed for RC columns strengthened by steel angles and strips that the load-bearing capacity can be evaluated by including the confinement effects on the uniaxial stress-strain law of the concrete to be used as input parameter. Yu *et al.* (2010) related the hardening/softening function to the plastic strain and the confining pressure of FRP-confined concrete as a field variable. Later, Hany *et al.* (2016) used the same approach introducing new findings regarding the path independency according to Ozbakkaloglu *et al.* (2016). For CFST-columns, Han *et al.* (2007) defined a stress-strain law for unconfined concrete to be used for FE analysis with ABAQUS software. Tao *et al.* (2013), also for CFST-columns, proposed a three-stage model to define the strain hardening/softening rule of concrete depending on the geometrical and mechanical parameters of the concrete and the steel tube.

In the present study, as a reference parameter, the mechanical transverse confinement ratio ω_{st} was considered to identify the confinement level of the steel composite

members

$$\omega_{st} = \omega_{st,x} + \omega_{st,y} \quad (10)$$

In doing so, K_c can be evaluated as

$$\omega_{st,x} = \frac{A_{st,x} f_{yb}}{h \cdot s_b f_{c0}}, \quad \omega_{st,y} = \frac{A_{st,y} f_{yb}}{b \cdot s_b f_{c0}} \quad (11)$$

In Eqs. (10) $A_{st,x}$ and $A_{st,y}$ are the area of the transverse steel bars along x and y direction respectively, b and h are the dimension of the concrete cross-section, s_b and f_{yb} are the spacing of the horizontal steel battens and the yielding stress, f_{c0} is the unconfined concrete strength.

The compressive response of concrete columns confined by steel jacketing reveals a “semi-active confinement” state of concrete. Differently from active or passive confinement, where confinement pressure is constant or variable throughout the load path, this is a hybrid situation between the two cases above mentioned. In the early stages of loading, the confining pressure is elastic up to the yielding of the external steel reinforcement (passive confinement).

Moreover, the non-uniform strain distribution along the height of the columns causes the yielding of the horizontal steel battens at different loading stages. Beyond the yielding of the steel, the concrete can be considered as “actively-confined”. The complex nature of this type of stress state for concrete requires an accurate definition of the hardening/softening function to be used in ABAQUS for CDP model.

In this study, the analytical model provided by Badalamenti *et al.* (2010) for concrete columns strengthened with steel angles and strips was used to generate, for given values of ω_{st} , a series of axial stress-strain curves of semi-active externally steel-confined concrete for the calibration of the numerical response obtained from ABAQUS with modification of the plasticity parameters for CDP model. In details, the dilation angle ψ and the hardening/function were considered depending on ω_{st} . By using the model of Badalamenti *et al.* (2010), the axial stress-strain relationship of the confined concrete can be obtained for each step of axial strain according to the model of Mander *et al.* (1988) but using a curve intertwining with several curves, each pertaining to a level of confining pressure corresponding to the current axial and lateral strain values.

Modifications of the analytical model were adopted to take into account the influences of the confining device on the lateral expansion of the concrete under axial compression. Differently from the authors that proposed to evaluate the lateral expansion of the concrete by Elwi and Murray (1979), in the present study the equation of Teng *et al.* (2007) is used for more reliable prediction of the lateral strain of concrete ε_l including also the lateral confinement pressure f_{le} as variable at each step of loading

$$\varepsilon_c = 0.85 \varepsilon_{c0} \left\{ \left[\left(1 + 8 \frac{f_{le}}{f_{c0}} \right) \left(1 - 0.75 \left(\frac{-\varepsilon_l}{\varepsilon_{c0}} \right) \right)^{0.7} - e^{\left(\frac{-\varepsilon_l}{\varepsilon_{c0}} \right)} \right] \right\} \quad (12)$$

In Eq. (11) ε_c is the current axial strain.

It should be noted that the relationship described above

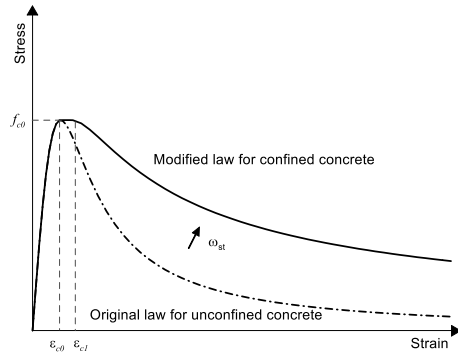


Fig. 4 Axial stress-strain response of steel angles in compression

refers to the sectional behavior of circular columns, therefore, in the present study, an equivalent circular section according to the assumption made by various authors such as Hany *et al.* (2016) is made. In this regard, equivalent diameter of the square cross-section was evaluated as

$$D_e = \sqrt{2}b \quad (13)$$

Accordingly, similar to Tao *et al.* (2013), a three stage model is used to represent the hardening/softening rule of concrete confined by steel angles and battens (Fig. 4). The first stage is obtained from the model for the stress-strain law of unconfined concrete provided by Popovics (1973) up to the reaching of the uniaxial compressive strength f_{c0} and the corresponding strain ϵ_{c0} . Beyond this point, increasing of strain at constant stress is defined up to the value ϵ_{c1} . Finally, the softening stage is still defined by the model of Popovics (1973) but replacing ϵ_{c0} with ϵ_{c1} .

In the proposed model, ϵ_{c1} is considered as the modified strain at the peak stress. This value should be adopted in the constitutive law of the unconfined concrete to modify the softening branch of the original law to take into account the effects of confinement. In this way, a slope of the softening is obtained depending on the mechanical transversal confinement ratio ω_{st} . The proposed model is therefore described by the following relationships

$$\frac{f_c(\epsilon)}{f_{c0}} = \begin{cases} \frac{x_1 \cdot \gamma_1}{\gamma_1 - 1 + x_1^{\gamma_1}} & 0 \leq \epsilon \leq \epsilon_{c0} \\ 1 & \epsilon_{c0} \leq \epsilon \leq \epsilon_{c1} \\ \frac{x_2 \cdot \gamma_2}{\gamma_2 - 1 + x_2^{\gamma_2}} & \epsilon \geq \epsilon_{c1} \end{cases} \quad (14)$$

$$\gamma_1 = \frac{E_c}{E_c - \frac{f_{c0}}{\epsilon_{c0}}}, \gamma_2 = \frac{E_c}{E_c - \frac{f_{c0}}{\epsilon_{c1}}}, x_1 = \frac{\epsilon}{\epsilon_{c0}}, x_2 = \frac{\epsilon}{\epsilon_{c1}} \quad (15)$$

The ratio between the strain ϵ_{c1} and the strain ϵ_{c0} and the dilation angle ψ were determined depending on ω_{st} by regression from numerical/analytical results (Figs. 5(a)-(b)).

Comparisons were also made with the model of Tao *et al.* (2013) proposed for CFST-columns. Regarding the dilation angle, it is worth nothing that the model proposed by Tao *et al.* (2013) concerned only fully steel-confined circular or square/rectangular concrete columns; to consider

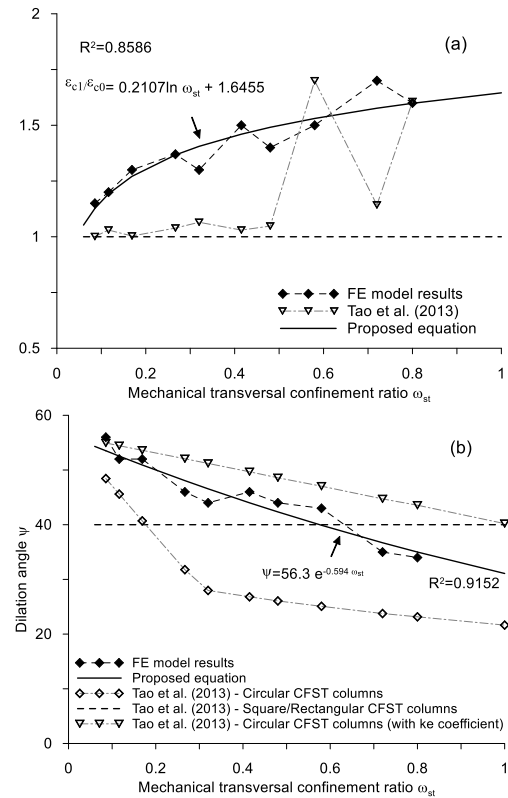


Fig. 5 Regression analysis of $\epsilon_{c1}/\epsilon_{c0}$ and ψ with respect to the mechanical transversal confinement ratio

the effect of discontinuous confinement as in the case of PSJ-columns the confinement effectiveness coefficients A_e/A_c in the plane of section and k_v along the height of the columns was adopted according to Hany *et al.* (2016) (for more details, refer to the original paper provided by the authors)

$$\frac{\epsilon_{c1}}{\epsilon_{c0}} = 0.2107 \cdot \ln(\omega_{st}) + 1.6455 \quad (16)$$

$$\psi = 56.3 e^{-0.594 \omega_{st}} \quad (17)$$

In Fig. 6 the axial stress-strain curves of the confined concrete obtained from the proposed model and the curves obtained from the analytical model of Badalamenti *et al.* (2010) with incorporating modifications are shown for different values of ω_{st} showing the reliability of the modification proposal for the plasticity parameters of the CDP model.

3. Verification of the proposed FE model

The performance of the proposed model is here validated against experimental results available in the literature. A comprehensive literature review of experimental specimens having a large range of mechanical transversal confinement ratio was collected for value of ω_{st} between 0.13 and 1.5.

Specimens of Adam *et al.* (2007), Giménez *et al.* (2009), Campione (2013), Tarabia and Albakry (2014), Belal *et al.*

Table 1 Summary of test data and FE comparisons

Source	ω_{st}	$P_{max,Exp}$ (kN)	$P_{max,FE}$ (kN)	$P_{max,FE}/P_{max,Exp}$	$P_{max,FE}$ (kN)	$P_{max,FE}/P_{max,Exp}$
			Default	Default	Proposed	Proposed
Adam <i>et al.</i> (2007)	0.526	2586.471	1951.484	0.754	2652.423	1.0254
	0.770	2338.208	1854.512	0.793	2374.309	1.0154
Giménez <i>et al.</i> (2009)	0.770	2186.757	1854.512	0.848	2374.309	1.0857
	0.130	745.415**	703.825	0.944	789.607	1.059
Campione (2013)	0.155	683.726**	683.726	0.881	654.31	0.957
	0.195	881.838**	766.703	0.869	854.190	0.969
Tarabia-Albakry (2014)	0.215	2334.670	2027.593	0.868	2301.318	0.985
	0.329	2356.816***	2206.089	0.936	2550.492	1.082
	0.400	2073.014***	1530.977	0.739	1778.05	0.858
Belal <i>et al.</i> (2015)	0.144	1828.706	1728.330	0.945	1929.756	1.055
	0.294	1642.580	1626.450	0.990	1991.105	1.212
	0.358	1847.499	1920.366	1.039	2026.240	1.096
Campione <i>et al.</i> (2017)	0.241	2439.500	2256.051	0.925	2543.370	1.042
	0.456	1875.733***	1749.480	0.933	1991.750	1.062
Shafei-Rahmdel (2017)*	0.515	42.978***	37.916	0.882	46.561	1.083
	1.473	50.520***	44.687	0.885	53.970	1.068

*Values in (MPa)

** Average between two specimens

*** Average between three specimens

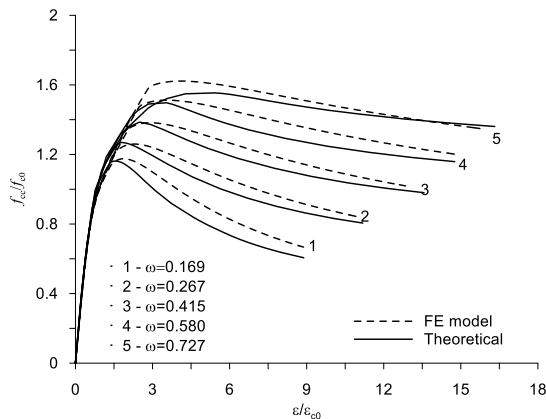


Fig. 6 Analytical and numerical stress-strain curves of semi-active confined concrete obtained from the proposed modification for CDP model

(2015), Shafei *et al.* (2017), Campione *et al.* (2017) were built with ABAQUS including the assessment concepts presented in the previous sections regarding the plasticity parameters for CDP model and compared with experimental results. In details, in each FE model built for the comparisons with experimental results, the ratio f_{bo}/f_{c0} , the parameter Kc , the modified hardening/softening rule and the dilation angle ψ are evaluated according to Eqs. (8)-(9), (13)-(16).

Details of the specimens are summarized in Table 1 coupled with the comparisons with the FE model in terms of ultimate compressive load. Moreover, the results of the analyses performed adopting the default values for the CDP model are reported for contrast with the FE results obtained by the proposed model.

Due to the minor or negligible influence of the internal steel reinforcement of some of the experimental specimens,

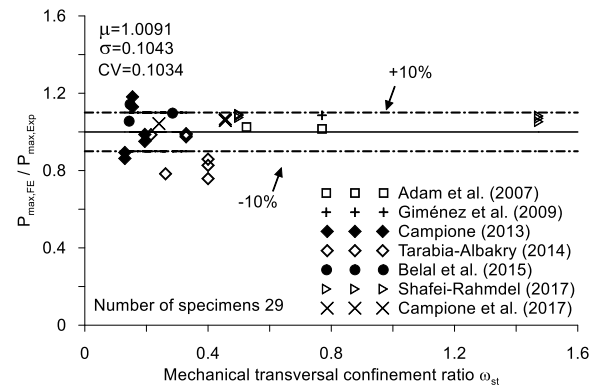


Fig. 7 FE predicted/Experimental results versus mechanical transversal confinement ratio

the value of ω_{st} was computed only depending on the external steel cage.

The prediction accuracy is confirmed in the range of the examined cases (a total of 29 tests were collected), showing the mean ratio between numerical and experimental results of 1.0114, standard deviation of 0.1079 and coefficient of variation of 0.1067. The average absolute error AAE was also computed returning a good reliable value of 8.828%. Comparisons between the ratio of the numerical and experimental maximum loads $P_{max,FE}/P_{max,Exp}$ are also illustrated in Fig. 7.

Some of the built models at failure are shown in Fig. 8 for illustrative purposes. It is worth noting that in most cases the FE models presented failure located at the same place of the experimental ones, confirming further the reliability of the model in predicting the physical behavior under compressive loads. Finally, the axial load-shortening/strain behavior was also compared with that provided by the experimental tests.

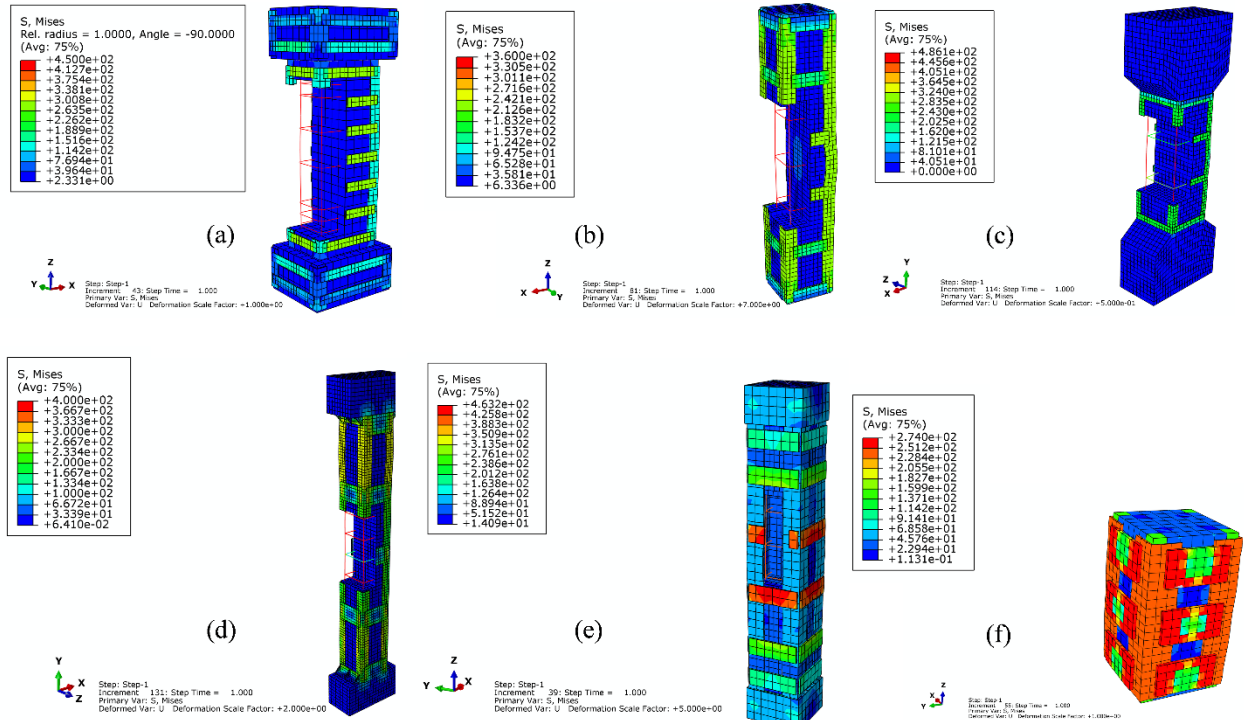


Fig. 8 FE models. Specimens RCA-B of Campione *et al.* (2017) (a); Specimen COL.01.4L.6P of Belal *et al.* (2015) (b); Specimen of Campione *et al.* (2013) (c); Specimen B of Adam *et al.* (2007); Specimens of Group 1 Tarabia *et al.* (2014) (e); Specimen NP3 of Shafei and Rahmdel (2017) (f)

The comparisons between the FE models and the experimental results (Fig. 9) show a very good agreement each other except for specimen COL.01.4L.6P of Belal *et al.* (2015) in which the FE model overestimated the experimental response. However, since the value of ω_{st} of the experimental specimens was 0.147 while the maximum load was lower than that of specimen COL.01.3L.6P with similar ω_{st} (0.144), probably anomalous behavior was obtained from the experimental test. Moreover, although in almost all the cases the strain at unconfined peak stress was evaluated through Eq. (6), for specimens RCA 1-3 of Campione *et al.* (2017), the value of ε_{c0} was assumed according to the authors since the differences between the analytical prediction and the experimental value presented a very large scatter (0.001359 obtained from Eq. (6) against 0.004 provided by the authors). As for the Table 1, the results of the FE analyses performed adopting the default values for the CDP model are shown in Fig. 9 to confirm the suitability of the modification proposal.

5. Conclusions

In this paper, concrete damaged plasticity model available in the software package ABAQUS was used to simulate the monotonic compressive behavior of partially steel-jacketed RC square and rectangular columns. A parametric study was carried out to evaluate the sensitivity of the plasticity parameters in the prediction of the load-bearing capacity of such strengthened columns before the introduction of appropriate modifications with respect to the

default values to be used in ABAQUS software.

A new hardening/softening function was defined coupled with the evaluation of the dilation angle depending on the mechanical transversal reinforcement ratio according to the theoretical model of Badalamenti *et al.* (2010).

The results of the proposed FE model were compared with experimental tests on specimens with a wide range of mechanical confinement ratios available in the literature. The comparisons showed a very good agreement in predicting both ultimate load and axial load-strain responses.

References

- ABAQUS (2013), ABAQUS Theory and User Manuals, Version 6.13-1.
- Adam, J.M., Ivorra, S., Giménez, E., Moragues, J.J., Mirigall, C. and Calderón, P.A. (2007), "Behaviour of axially loaded RC columns strengthened by steel angles and strips", *Steel Compos. Struct.*, **7**(5), 405-419.
- Badalamenti, V., Campione, G. and Mangiavillano, M.L. (2010), "Simplified model for compressive behavior of concrete columns strengthened by steel angles and strips", *J. Eng. Mech.*, ASCE, **136**(2), 230-238.
- Barasan, H. (2015), "Dynamic behavior investigation of scale building renovated by repair mortar", *Comput. Concrete*, **16**(4), 531-544.
- Behfarnia, K. and Shirmeshan, S. (2017), "A numerical study on behavior of CFRP strengthened shear wall with opening", *Comput. Concrete*, **19**(2), 179-189.
- Belal, M.F., Mohamed, H.M. and Morad, S.A. (2015), "Behavior of reinforced concrete columns strengthened by steel jacket",

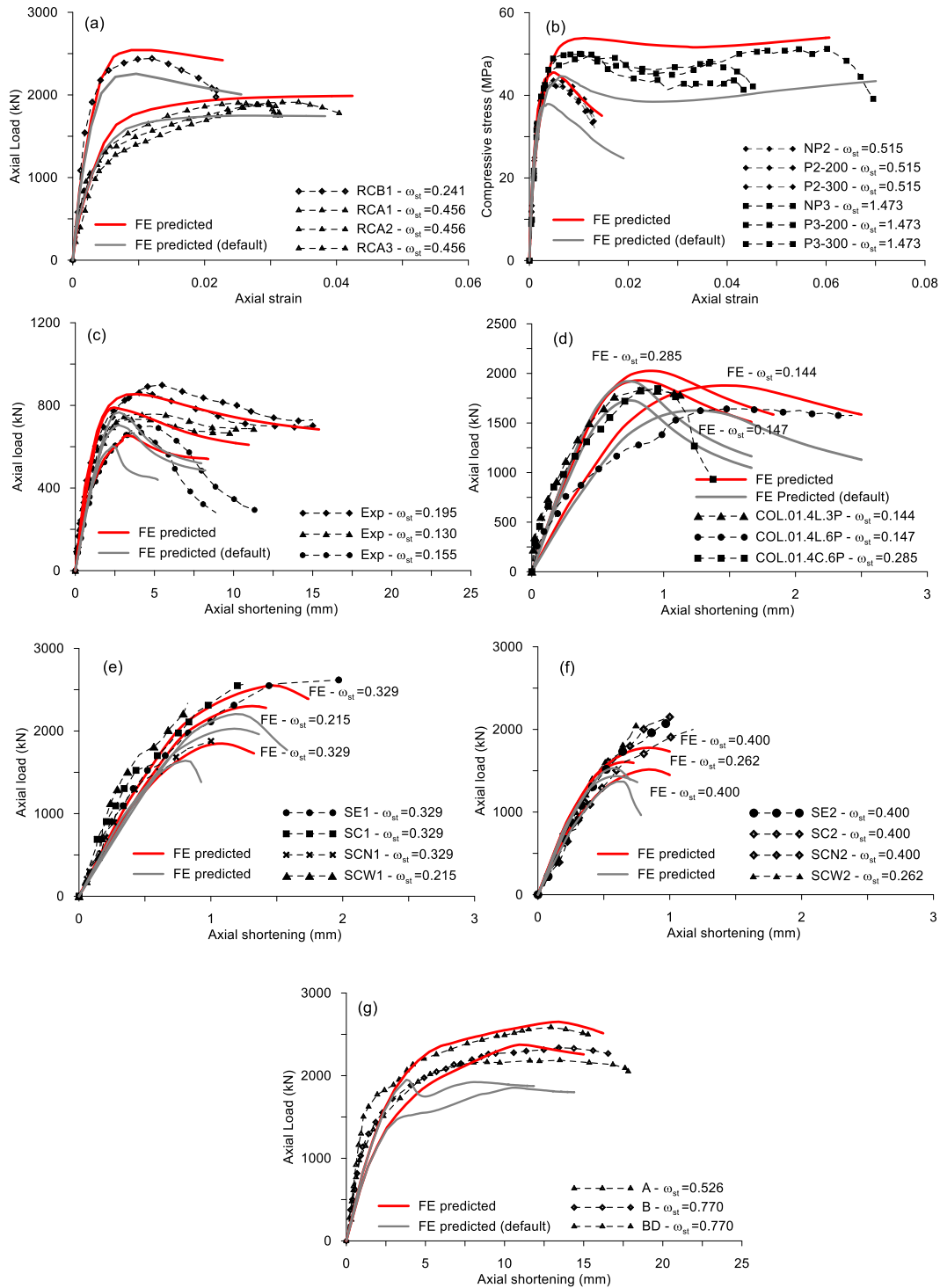


Fig. 9 Comparisons between FE predictions and experimental data. Campione *et al.* (2017) (a); Shafei and Rahmdel (2017) (b); Campione (2013) (c); Belal *et al.* (2015) (d); Tarabia and Albakry (2014) - Group 1 (e) and Group 2 (f); Adam *et al.* (2007) and Giménez *et al.* (2009) (g)

HBRC J., **11**, 201-212.
 Campione, G. (2013), "RC columns strengthened with steel angles and battens: Experimental results and design procedure", *Pract. Period. Struct. Des. Constr.*, ASCE, **18**(1), 1-11.
 Campione, G., Cavaleri, L., Di Trapani, F. and Ferrotto, M.F. (2017), "Frictional effects on structural behavior of no-end-connected steel-jacketed RC columns: Experimental results and new approaches to model numerical and analytical response", *J. Struct. Eng.*, ASCE, **143**(8), 04017070.

Campione, G., Cavaleri, L., Ferrotto, M.F., Macaluso, G. and Papia, M. (2016), "Efficiency of stress-strain models of confined concrete with and without steel jacketing to reproduce experimental results", *Open Constr. Build. Technol. J.*, **10** (Suppl 1: M4), 65-86.
 Cavaleri, L., Di Trapani, F., Ferrotto, M.F. and Davì, L. (2017), "Stress-strain models for normal and high strength confined concrete: Test and comparisons of literature models reliability in reproducing experimental results", *Ingegneria Sismica*, **34**(

- Special Issue B), 114-137.
- Chen, Y., Feng, J. and Yin, S. (2012), "Compressive behavior of reinforced concrete columns confined by multi-spiral hoops", *Comput. Concrete*, **9**(5), 359-373.
- Chen, Y., Sareh, P. and Feng, J. (2015), "Effective insights into the geometric stability of symmetric skeletal structures under symmetric variations", *Int. J. Solid. Struct.*, **69**, 277-290.
- Chen, Y., Sareh, P., Feng, J. and Sun, Q. (2017), "A computational method for automated detection of engineering structures with cyclic symmetries", *Comput. Struct.*, **191**, 153-164.
- Chi, Y., Yu, M., Huang, L. and Xu, L. (2017), "Finite element modeling of steel-polypropylene hybrid fiber reinforced concrete using modified concrete damaged plasticity", *Eng. Struct.*, **148**, 23-35.
- Elwi, A.A. and Murray, D.W. (1979), "A 3D hypoelastic concrete constitutive relationship", *J. Eng. Mech.*, **105**, 623-641.
- Ferrotto, M.F., Fischer, O. and Niedermeier, R. (2017), "Experimental investigation on the compressive behavior of short-term preloaded carbon fiber reinforced polymer-confined concrete columns", *Struct. Concrete*. DOI: 10.1002/suco.201700072.
- Genikomsou, A.S. and Polak, M.A. (2015), "Finite element analysis of punching shear of concrete slabs using damaged plasticity model in ABAQUS", *Eng. Struct.*, **98**, 38-48.
- Giménez, E., Adam, J.M., Ivorra, S., Moragues, J.J. and Calderón, P.A. (2009), "Full-scale testing of axially loaded RC columns strengthened by steel angles and strips", *Adv. Struct. Eng.*, **12**(9), 169-181.
- Gupta, P., Verma, V.K., Kubba, Z. and Singh, H. (2015), "Effect of tube area on the behavior of concrete filled tubular columns", *Comput. Concrete*, **15**(2), 141-166.
- Han, L.H., Yao, G.H. and Tao, Z. (2007), "Performance of concrete-filled thin-walled steel tubes under pure torsion", *Thin Wall. Struct.*, **45**, 24-36.
- Hany, N.F., Hantouche, E.G. and Harajli, M.H. (2016), "Finite element modeling of FRP-confined concrete using modified concrete damaged plasticity", *Eng. Struct.*, **125**, 1-14.
- Hoang, A.L. and Fehling, E. (2017), "Numerical analysis of circular steel tube confined UHPC stub columns", *Comput. Concrete*, **19**(3), 263-273.
- Jin, N., Tian, Y. and Jin, X. (2007), "Numerical simulation of fracture and damage behaviour of concrete at different ages", *Comput. Concrete*, **4**(3), 221-241.
- Mahdikhani, M., Naderi, M. and Zekavati, M. (2016), "Finite element modeling of the influence of FRP techniques on the seismic behavior of historical arch stone bridge", *Comput. Concrete*, **18**(1), 99-112.
- Mander, J.B., Priestley, M.J. and Park, R.N. (1988), "Theoretical Stress-Strain Model for Confined Concrete", *J. Struct. Eng.*, ASCE, **114**(8), 1804-1826.
- Ozbakkaloglu, T., Gholampour, A. and Lim, J.C. (2016), "Damage-plasticity model for FRP-confined normal-strength and high-strength concrete", *J. Compos. Constr.* ASCE, **20**(6), 04016053.
- Papanikolaou, V.K. and Kappos, A.J. (2007), "Confinement-sensitive plasticity constitutive model for concrete in triaxial compression", *Solid. Struct.*, **44**(21), 7021-7048.
- Popovics, S. (1973), "A numerical approach to the complete stress-strain curve of concrete", *Cement Concrete Res.*, **3**(5), 583-599.
- Shafei, E. and Rahmdel, J.M. (2017), "Plasticity constitutive modeling of partially confined concrete with steel jacketing", *KSCE J. Civ. Eng.*, **21**(7), 2738-2750.
- Tao, Z., Wang, Z.B. and Yu, Q. (2013), "Finite element modelling of concrete-filled steel stub columns under axial compression", *J. Constr. Steel Res.*, **89**, 121-131.
- Tarabia, A.M. and Albakry, H.F. (2014), "Strengthening of RC columns by steel angles and strips", *Alexandria Eng. J.*, **53**, 615-626.
- Teng, J.G., Huang, Y.L., Lam, L. and Ye, L.P. (2007), "Theoretical model for fiber-reinforced polymer-confined cConcrete", *J. Compos. Constr.*, ASCE, **11**, 201-210.
- Yu, T., Teng, J.G., Wong, Y.L. and Dong, S.L. (2010), "Finite element modeling of confined concrete-II: Plastic-damage model", *Eng. Struct.*, **32**, 680-591.

CC